ELSEVIER

Journal of Biomechanics 36 (2003) 19–34

JOURNAL OF BIOMECHANICS

www.elsevier.com/locate/jbiomech
www.JBiomech.com

How the stiffness of meniscal attachments and meniscal material properties affect tibio-femoral contact pressure computed using a validated finite element model of the human knee joint

Tammy L. Haut Donahue[a,e,*], M.L. Hull[a,b], Mark M. Rashid[c], Christopher R. Jacobs[d]

[a] *Biomedical Engineering Program, University of California at Davis, Davis, CA 95616, USA*
[b] *Department of Mechanical Engineering, University of California at Davis, Davis, CA 95616, USA*
[c] *Department of Civil Engineering, University of California at Davis, Davis, CA 95616, USA*
[d] *Department of Mechanical Engineering, Stanford University, Stanford, CA 94305, USA*
[e] *Department of Mechanical Engineering—Engineering Mechanics, Michigan Technological University, 1400 Townsend Dr., Houghton, MI 49931, USA*

Accepted 22 August 2002

Abstract

In an effort to prevent degeneration of articular cartilage associated with meniscectomies, both meniscal allografts and synthetic replacements are subjects of current interest and investigation. The objectives of the current study were to (1) determine whether a transversely isotropic, linearly elastic, homogeneous material model of the meniscal tissue is necessary to achieve a normal contact pressure distribution on the tibial plateau, (2) determine which material and boundary condition (attachments) parameters affect the contact pressure distribution most strongly, and (3) set tolerances on these parameters to restore the contact pressure distribution to within a specified error. To satisfy these objectives, a finite element model of the tibio-femoral joint of a human cadaveric knee (including both menisci) was used to study the contact pressure distribution on the tibial plateau. To validate the model, the contact pressure distribution on the tibial plateau was measured experimentally in the same knee used to create the model. Within physiologically reasonable bounds on five material parameters and four attachment parameters associated with a meniscal replacement, an optimization was performed under 1200 N of compressive load on the set of nine parameters to minimize the difference between the experimental and model results. The error between the experimental and model contact variables was minimized to 5.4%. The contact pressure distribution of the tibial plateau was sensitive to the circumferential modulus, axial/radial modulus, and horn stiffness, but relatively insensitive to the remaining six parameters. Consequently, both the circumferential and axial/radial moduli are important determinants of the contact pressure distribution, and hence should be matched in the design and/or selection of meniscal replacements. In addition, during surgical implantation of a meniscal replacement, the horns should be attached with high stiffness bone plugs, and the attachments of the transverse ligament and deep medial collateral ligament should be restored to minimize changes in the contact pressure distribution, and thereby possibly prevent the degradation of articular cartilage.
© 2002 Elsevier Science Ltd. All rights reserved.

Keywords: Meniscus; Contact; Finite element method; Material properties; Knee

1. Introduction

In an effort to prevent degeneration of the articular cartilage caused by meniscectomies (Bolano and Grana, 1993; Fauno and Nielson, 1992; Rangger et al., 1995), both meniscal allografts (De Boer and Koudstaal, 1991; Siegel and Roberts, 1993; Stone, 1993;Veltri et al., 1994) and synthetic replacements (Kollias and Fox, 1996; Messner, 1994; Stone et al., 1992) have been previously investigated. However, the clinical success of meniscal allografts has been varied (Arnoczky et al., 1990; De Boer and Koudstaal, 1991; Garrett and Stevensen, 1991; Jackson et al., 1992; Kohn et al., 1992; Mikic et al.,

*Corresponding author. Department of Mechanical Engineering, Michigan Technological University, 1400 Townsend Dr., Houghton, MI 49931, USA. Tel.: +1-906-487-2078; fax: +1-906-487-2822.
E-mail address: thdonahu@mtu.edu (T.L. Haut Donahue).

0021-9290/02/$ - see front matter © 2002 Elsevier Science Ltd. All rights reserved.
PII: S0021-9290(02)00305-6

1993; Milachowski et al., 1989). The mixed results may be due in part to a failure of the replacement to satisfy the biomechanical criteria necessary for proper meniscal function.

Among the most important biomechanical factors that determine the relative success of a meniscal replacement are the material properties of the tissue. Meniscal collagen fibers are arranged predominantly in the circumferential direction. These fibers function to support the large hoop stresses that are important to the distribution of contact pressures within the knee joint. Previous studies have demonstrated that the radial modulus is influenced by the presence of radial tie fibers (Skaggs et al., 1994); however, the modulus in the radial and axial directions is approximately 10 times less than that of the circumferential direction (Tissakht and Ahmed, 1995). Therefore, it appears that a transversely isotropic constitutive relationship is appropriate to represent the meniscal tissue. Mathematical models of load transmission of the tibio-femoral joint, which have modeled the meniscus as transversely isotropic, suggest that the circumferential tensile modulus is critical to achieving proper distribution of contact pressure (Schreppers et al., 1990; Spilker and Donzelli, 1992). However, a transversely isotropic constitutive relation requires five independent parameters, and the relative importance of the remaining four parameters, in addition to the circumferential modulus, on the contact pressure distribution is at the present unknown.

Another factor that may be important to the success of meniscal replacements is the attachment of the meniscus to the surrounding tissues. The anterior and posterior horns of each meniscus are connected to the tibial plateau either by means of ligaments or by direct insertion (Arnoczky et al., 1987). In addition, the posterior fibers of the anterior horn of the medial meniscus merge with the transverse ligament, which then connects to the anterior horn of the lateral meniscus. The medial meniscus is more firmly attached than the lateral meniscus to the femur and tibia by a thickening in the joint capsule known as the deep medial collateral ligament (MCL). While the function of these various attachments is to provide restraints that limit the relative movement of the meniscus on the tibial plateau when it bears load (Tissakht et al., 1989), the relative importance of each attachment on the contact pressure distribution is at present unknown.

Currently, tissue banks do not consider material properties in selecting meniscal allografts, and those developing synthetic replacements are not guided by any design criteria for restoring meniscal function. In addition, during meniscal replacement surgery, a question that remains to be answered is what specific attachments must be restored since attaching the horns alone does not restore normal meniscal function (Alhalki et al., 1999). Therefore, the objectives of the current study were to (1) determine whether a transversely isotropic, linearly elastic, homogeneous constitutive relationship is necessary to achieve a normal contact pressure distribution on the tibial plateau, (2) determine material parameters and attachment parameters to which the contact pressure distribution of the tibial plateau is most sensitive, and (3) determine tolerances on material and attachment parameters that will restore the contact pressure distribution to within a specified difference from normal.

2. Methods

2.1. Determination of experimental contact variables

One human, fresh-frozen, cadaveric, right knee was obtained from a 30-year-old male. Antero-posterior and lateral roentgenograms of the knee were obtained to ensure that there was no joint space narrowing, osteophytes, chondrocalcinosis, meniscal tears, or history of knee surgery. The knee was then aligned in a specialized load application system for the testing of joints (Bach and Hull, 1995). The knee was aligned using a functional-axes approach, which has been shown to exhibit good repeatability (Berns et al., 1990). To implement this approach, the tibia and femur were each placed inside alignment fixtures that allowed for a six degree-of-freedom adjustment so that the natural rotational axes of the joint were aligned with the rotational axes of the load application system.

Contact pressure distributions were measured on the same knee that was ultimately modeled using finite elements. Two ranges of pressure-sensitive film were used in this study: super-low- and low-range pressure film (Fuji Prescale Film; C Itoh, New York, NY) (Huang et al., 2002; Paletta et al., 1997). Pressure-sensitive film packets were created for the knee to match both the size and shape of the lateral and medial tibial plateaus using a previously described technique (Alhalki et al., 1999; Martens et al., 1997).

The load application system constrained flexion at a predetermined angle while applying compressive loads. Relative motions between the tibia and femur were unconstrained in all other degrees of freedom. The contact pressure distribution of the knee was measured with the pressure-sensitive film as compressive load was applied using the load application system. Three factors were controlled during the exposure of the pressure sensitive film: shear, overshoot, and loading time (Martens et al., 1997). Orientation of the film on the tibial plateau was recorded by placing registration marks on the film in regions that supported only minimal load (Huberti and Hayes, 1984). Two registration marks were placed on each of the lateral and medial tibial plateaus. Three repetitions, each with new pressure

film, were made at 0 and 15 degrees of flexion under compressive loads of 400 and 1200 N. These load levels represented $\frac{1}{2}$ and $1\frac{1}{2}$ times body weight, respectively. Contact data were recorded for both the medial and lateral tibial plateaus.

After joint contact pressure distributions were recorded with the pressure-sensitive film, two metal rods were drilled through the knee penetrating both the femur and the tibia while the joint was held at 0 degrees of flexion. This served to define the 'reference position' of the knee. The rods were then removed and replaced with delrin rods which served as alignment markers for reconstruction of the 3-dimensional (3-D) geometry later in the study.

To convert the intensity of the film stain to a pressure value, calibration curves were generated for both the super-low-range film, and the low-range film using a previously established procedure (Alhalki et al., 1999; Liggins et al., 1995; Liggins et al., 1992; Martens et al., 1997). The maximum pressure, contact area, mean pressure, and the location of the maximum pressure (collectively termed the contact variables) were determined from the calibrated images.

The contact variables were determined using both ranges of film. The maximum pressure was determined by averaging the maximum pressure from the three trials using only the low-range film. The location of the maximum pressure was measured on the low-range film, and using registration markers, the location was transferred to a global anatomical coordinate system. The global coordinate system was established by first drawing a line parallel to the posterior osteochondral junction of the proximal tibia to define the medial–lateral (M/L) direction. The anterior–posterior (A/P) direction was defined as perpendicular to this line. The origin was placed at half the maximum A/P distance and half the maximum M/L distance. The location of maximum pressure was determined by averaging the location from the three trials. The total contact area was determined by averaging the contact area from the three trials using only the super-low-range film. Lastly, the mean pressure for a trial was obtained using a combination of both the super-low- and low-range pressure films (See Appendix A). The final mean pressure was determined by averaging the mean pressure from the three trials.

2.2. Creation of the finite element model

A finite element model of the cadaveric knee joint was created as previously described (Haut Donahue et al., 2002) (Fig. 1). Briefly, a finite model was generated from a 3-D laser coordinate digitizing system (Haut et al., 1997) that imaged the cartilage and menisci with an error of less than 8 μm. This digitizing system attempts to minimize the effects of dehydration of the exposed tissue (Haut et al., 1997). The model included both the femoral and tibial articular cartilage, both the medial and lateral menisci and their horn attachments, the anterior cruciate ligament, the transverse ligament, and the deep medial collateral ligament. The bones were treated as rigid because a previous study confirmed that this simplification had no substantive effect on the contact variables (Haut Donahue et al., 2002). The cartilage was considered as linearly elastic and isotropic with an elastic modulus of 15 MPa and a Poisson's ratio of 0.475 (Table 1), maintaining the nearly incompressible behavior of the cartilage tissue under short loading times. The anterior cruciate and deep medial collateral ligaments were modeled as 1-D nonlinear springs (Blankevoort et al., 1991; Li et al., 1999; Pandy et al., 1997; Wismans et al., 1980), requiring a nonlinear

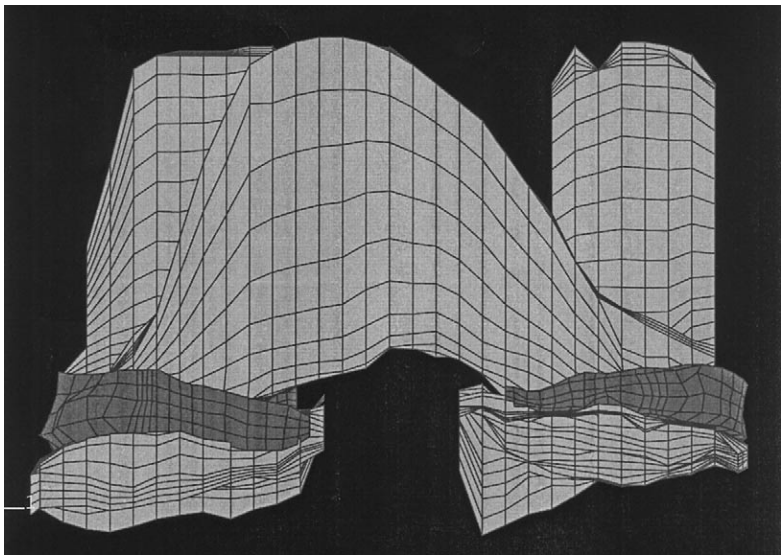

Fig. 1. Finite element representation of the knee joint.

stiffness parameter (k), and a reference strain (ε_r), where reference strain is the initial strain in the reference position (i.e. full extension) (Fig. 2). The following 1-D nonlinear relationship was employed:

$$\begin{aligned} f &= k(\varepsilon - \varepsilon_1) && \text{if} \quad \varepsilon \geqslant 2\varepsilon_1, \\ f &= 1/4k(\varepsilon^2/\varepsilon_1) && \text{if} \quad 0.0 < \varepsilon < 2\varepsilon_1, \\ f &= 0 && \text{if} \quad \varepsilon \leqslant 0.0, \end{aligned} \tag{1}$$

Table 1
Material properties of modeled tissues not included in the optimization

Femoral/tibial cartilage	Linearly elastic, isotropic	$E = 15$ MPa, $\nu = 0.475$
ACL	1-D nonlinear spring	Anterior bundle; Ref. strain = 0.06 mm/mm Nonlinear stiffness = 5000 N Posterior bundle; Ref. strain = 0.10 mm/mm Nonlinear stiffness = 5000 N

where ε_l is the nonlinear strain level parameter assumed to be 0.03 as in previous studies (Butler et al., 1986; Li et al., 1999; Pandy et al., 1997). Both of these ligaments were modeled with anterior and posterior bundles. The transverse ligament and horn attachments were modeled as linear springs.

The general-purpose finite element code ABAQUS (HKS Inc., Pawtucket, RI) was used to obtain finite element solutions to the contact problem. The articular cartilage and menisci were discretized into 8-node trilinear hexahedral elements. Contact was modeled between the femur and meniscus, the meniscus and tibia, and the femur and tibia for both the lateral and medial compartments, resulting in six contact-surface pairs. The contact conditions in the model were completely general involving finite sliding of pairs of curved, deformable surfaces. All of the surfaces were modeled as frictionless. A convergence analysis demonstrated that the finite element solution converged for a mesh that had an average element size of 2 mm × 2 mm and

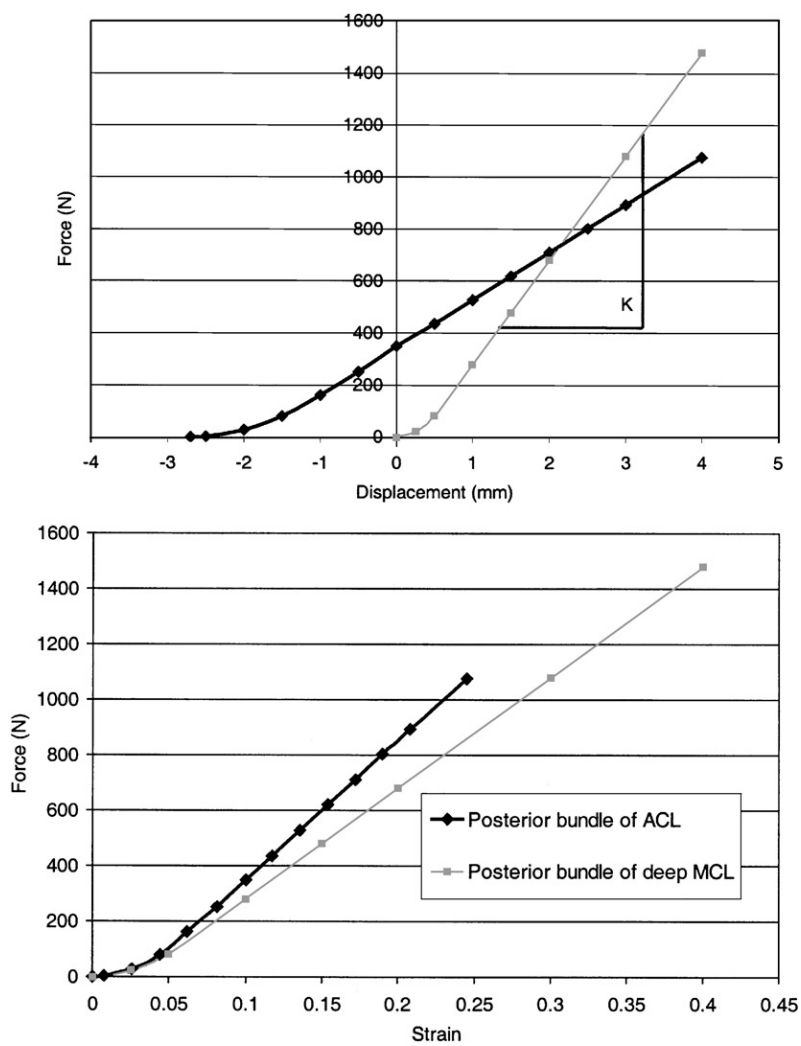

Fig. 2. (a) Nonlinear force versus displacement curves and (b) nonlinear force versus strain curves for the posterior bundle of the ACL and the posterior bundle of the deep MCL.

consisted of 14,050 total elements: 2500 meniscal elements in four layers, 3000 femoral cartilage elements in four layers, 2500 tibia cartilage elements in four layers. See Haut Donahue et al. (2002) for additional details of the finite element model (Haut Donahue et al., 2002).

The model was compressed to a load level of 1200 N at 0 degrees of flexion and the same contact variables that were determined experimentally were determined from the model solution. For the calculation of contact area and mean pressure from the model, pressures below 0.25 MPa were set to 0.0 MPa because 0.25 MPa was the threshold pressure below which the super-low-range film would not register any reading.

To perform an optimization, an error measure was defined to quantify differences between the contact variables determined experimentally and those computed with the model. The root-mean-square normalized error (RMSNE) was calculated as

$$\mathrm{RMSNE} = \sqrt{\frac{\sum_{i=1}^{m}(\mathrm{Error}_i)^2}{m}}, \quad \text{where } m = 4 \tag{2}$$

and

$$\mathrm{Error}_i^2 = \left(\frac{X_{\mathrm{measured},i} - X_{\mathrm{model},i}}{X_{\mathrm{measured},i}}\right)^2_{\mathrm{lateral}} + \left(\frac{X_{\mathrm{measured},i} - X_{\mathrm{model},i}}{X_{\mathrm{measured},i}}\right)^2_{\mathrm{medial}}, \tag{3}$$

where the reference values for $X_{\mathrm{measured},i}$ were determined from the experimental data and the values for $X_{\mathrm{model},i}$ were computed from the finite element model. So that the location of maximum pressure was given equal weighting to the mean pressure, maximum pressure, and contact area, the M/L and A/P locations of the maximum pressure were combined by weighting each 50% to combine them into one quantity.

2.3. Optimization/sensitivity analysis

A multivariable optimization was performed on the set of nine material and attachment parameters associated with a meniscal replacement to minimize the RMSNE. The nine parameters included the following: (1) the shear modulus ($G_{r\theta} = G_{z\theta}$), (2) the stiffness of the transverse ligament, (3) the stiffness of the horn attachments, (4) the nonlinear stiffness parameter for the deep MCL, (5) the reference strain for the deep MCL, (6) the out-of-plane Poisson ratios ($\nu_{r\theta} = \nu_{z\theta}$), (7) the in-plane Poisson ratio (ν_{rz}), (8) the axial/radial modulus ($E_z = E_r$), and (9) the circumferential modulus (E_θ). Note that for the purposes of the optimization and sensitivity analyses, the two bundles of the deep medial collateral ligament were given the same parameter values. The initial values and ranges of the parameter values for the optimization were:

1. $G_{r\theta} = G_{z\theta} = 57.7$ MPa (range 27.7–77.7 MPa),
2. stiffness of transverse ligament = 200 N/mm (1 spring) (range 50–900 N/mm),
3. total stiffness of horn attachment = 2000 N/mm (10 springs/horn × 200 N/mm) (range 500–30,000 N/mm),
4. nonlinear stiffness of medial collateral ligament bundles = 2000 N (range 500–5000 N; from Blankevoort et al., 1991; Li et al., 1999; Pandy et al., 1997; Wismans et al., 1980),
5. reference strain of medial collateral ligament bundles = 0.08 (range –0.08–2.4; from Blankevoort et al., 1991; Li et al., 1999; Pandy et al., 1997; Wismans et al., 1980),
6. $\nu_{r\theta} = \nu_{z\theta} = 0.3$ (range 0.1–0.35, to satisfy stability requirements with a transversely isotropic model),
7. $\nu_{rz} = 0.2$ (range 0.1–0.4),
8. $E_r = E_z = 20$ MPa (range 15–60 MPa; from Skaggs et al., 1994; Tissakht and Ahmed, 1995; Whipple et al., 1984),
9. $E_\theta = 150$ MPa (range 100–200 MPa; from Fithian et al., 1989; Tissakht and Ahmed, 1995;Whipple et al., 1984).

The initial value and range for each of the parameters were determined from either the literature or from stability requirements, in the case of the Poisson ratios. However, neither the shear modulus nor the stiffness of the transverse ligament and horn attachments were available from the literature. The initial value for the shear modulus was calculated by assuming elastic isotropy, with a Poisson ratio of 0.3 and a modulus of 150 MPa. The range was then calculated as ±50% of the initial value. Since most of the horns attach via a ligament, the initial stiffness for the transverse ligament and horns was derived from the modulus of the ACL. The length of the transverse ligament was approximately 30 mm as measured with a scale during dissection, and the cross-sectional area was approximately 20 mm^2 as determined from the reconstructed model. Therefore, using the modulus of 111 ± 26 MPa (Noyes and Grood, 1976), the initial stiffness value for the transverse ligament was approximated to be 200 N/mm. The range encompassed at least two standard deviations about this value. The same initial value was used for a single spring of the horn attachments, resulting in a total horn stiffness of 2000 N/mm. The total horn stiffness was varied over a range encompassing values as low as that corresponding to sutures (50 N/mm) to as high as a relatively rigid bone attachment (30,000 N/mm).

Considering the complexity of a linearly elastic and transversely isotropic constitutive relation for the meniscal tissue, it was of interest to determine whether the meniscal material could be considered as linearly

elastic and isotropic. Accordingly, the RMSNE was computed while the elastic modulus and Poisson's ratio were varied from 50 to 200 MPa and 0.1 to 0.49, respectively, and the remaining parameters remained constant at their values given above from the literature.

To optimize the nine parameters, a semi-automated technique was used. First, the model was run with these nine parameters set to their initial values. Then, while leaving the remaining eight parameters set to their initial values, the shear modulus ($G_{r\theta} = G_{z\theta}$) was varied over a range from 27.7 to 77.7 MPa. Six values of shear modulus, over the range indicated, were evaluated. Of these six values, the value of the shear modulus that minimized the RMSNE was determined. Next, with the shear modulus set at the value that minimized the error, the stiffness of the transverse ligament was varied over a range from 50 to 900 N/mm, while the remaining seven parameters were left at their initial values. Again, as for the shear modulus, the RMSNE was minimized and the resulting value for the transverse ligament stiffness was determined. The process was continued until all nine parameters were examined.

The optimization was repeated with a different set of initial values to check if the minimum reached in the first optimization was in fact a global minimum. The initial values were randomly selected for the second optimization and were as follows:

1. $G_{r\theta} = G_{z\theta} = 37.7$ MPa,
2. stiffness of transverse ligament = 500 N/mm (1 spring),
3. total stiffness of horn attachment = 6000 N/mm,
4. nonlinear stiffness of medial collateral ligament bundles = 4000 N,
5. reference strain of medial collateral ligament bundles = −0.08,
6. $\nu_{r\theta} = \nu_{z\theta} = 0.2$,
7. $\nu_{rz} = 0.4$,
8. $E_r = E_z = 40$ MPa,
9. $E_\theta = 200$ MPa.

The same optimization technique was used again to minimize the error function over the same ranges of the parameter values.

The second optimization revealed differences in final values for three of the parameters, whereas the optimal values of the other six parameters were the same as those obtained in the first optimization. These three parameters were also the most sensitive parameters as determined by the change in RMSNE value over the range studied (larger than a 5% change in RMSNE was considered sensitive). A grid search was performed with these three parameters while holding the remaining six parameters at their optimized values. The grid search served the dual purpose of determining a globally optimal set of parameters, while also determining tolerances on the three most sensitive parameters that would lead to an acceptable meniscal replacement. The three most sensitive parameters included the stiffness of the horn attachments, the axial/radial modulus, and the circumferential modulus. The grid search used four values for the total stiffness of the horn attachments (500, 2000, 6000, 10,000 N/mm), four values for the axial/radial modulus (15, 20, 40, 60 MPa), and three values for the circumferential modulus (100, 150, 200 MPa). A finite element analysis was performed for each of the 48 different factorial combinations (i.e. $4 \times 4 \times 3 = 48$). The ranges used for the axial/radial modulus and the circumferential modulus corresponded to their physiological ranges. The lower limit for the total stiffness of the horn attachments was the value from the first and second optimizations that resulted in an RMSNE less than 20%. The upper limit for this parameter was set to 10,000 N/mm. This value was reduced from the upper limit of the range used in the first and second optimizations because there was no change in the RMSNE during the optimizations when the horn stiffness was greater than 10,000 N/mm.

Lastly, for an independent validation of the model, the model was compressed to 400 N at 15 degrees of flexion using the set of parameter values that provided the minimum RMSNE when the model was compressed to 1200 N at 0 degrees of flexion. The RMSNE was calculated at 400 N and 15 degrees of flexion to compare the computed contact variables to those determined experimentally at 400 N and 15 degrees of flexion.

3. Results

When the constitutive relation for the meniscal material was considered to be transversely isotropic, an RMSNE of 5.4% was obtained by the first optimization (Table 2). The minimization resulted in values for each of the nine parameters as follows:

1. $G_{r\theta} = G_{z\theta} = 57.7$ MPa,
2. stiffness of transverse ligament = 900 N/mm,
3. total stiffness of horn attachment = 2000 N/mm,
4. nonlinear stiffness of medial collateral ligament bundles = 4000 N,
5. reference strain of medial collateral ligament bundles = 0.00,
6. $\nu_{r\theta} = \nu_{z\theta} = 0.3$,
7. $\nu_{rz} = 0.2$,
8. $E_r = E_z = 20$ MPa,
9. $E_\theta = 150$ MPa.

The second optimization, which achieved an RMSNE of 6.9%, resulted in different parameter values from those of the first optimization for the total stiffness of the horn attachment (6000 N/mm), the radial/axial modulus ($E_r = E_z = 40$ MPa), and the circumferential modulus ($E_\theta = 200$ MPa). Although the different results between the two semi-automated optimizations

Table 2
Contact variables from experimental data and the first optimization (RMSNE = 5.4%). Anterior and medial are positive for the A/P and M/L locations of maximum pressure, respectively

	Max. pressure (MPa)	Mean pressure (MPa)	Area (mm^2)	A/P location max. pressure (mm)	M/L location max. pressure (mm)
Lateral-experimental	3.78	1.53	384.8	5.6	−17.6
Lateral-model	3.69	1.59	378.0	5.4	−16.2
Medial-experimental	3.46	1.42	372.0	−3.0	18.9
Medial-model	3.44	1.36	360.0	−1.6	19.5

Table 3
RMSNE values for the grid search

Circumferential modulus (MPa)/Horn stiffness (N/mm)	15 MPa	20 MPa	40 MPa	60 MPa
	Axial/radial modulus			
100/500	0.210	0.124	0.120	0.117
150/500	0.233	**0.096**	0.103	0.117
200/500	XX	0.246	0.113	0.123
100/2000	0.102	**0.092**	0.172	0.106
150/2000	0.220	**0.054**	**0.095**	0.109
200/2000	XX	0.226	**0.076**	0.113
100/6000	0.264	0.148	**0.096**	**0.073**
150/6000	0.272	0.202	**0.078**	**0.089**
200/6000	XX	0.203	**0.069**	**0.099**
100/10,000	0.242	0.101	**0.099**	**0.070**
150/10,000	0.258	**0.057**	**0.091**	**0.086**
200/10,000	XX	0.219	**0.065**	**0.095**

XX—these combinations were not possible with a transversely isotropic constitutive relation with an in-plane Poisson's ratio of 0.2 and out-of-plane ratio of 0.3.
Values in bold type represent RMSNE less than 10%.

suggested that the 5.4% RMSNE value obtained in the first optimization may not be the global minimum, the subsequent grid search revealed that the final parameter values in the first optimization did indeed provide the global minimum (Table 3).

The results of the semi-automated optimizations suggested not only a significant interaction between the total horn stiffness, the axial/radial modulus, and circumferential modulus, but also indicated that the RMSNE was most sensitive to these three parameters (Fig. 3). Variations in each of these parameters over the range studied increased the RMSNE by more than 5%. The contact variables were not sensitive to the remaining six parameters in either the first or second semi-automated optimization (Fig. 4) for the ranges studied.

When examining how variations in the three most sensitive parameters affected the contact variables, the maximum pressure, mean pressure, and contact area were affected to a greater degree on the lateral tibial plateau than on the medial tibial plateau. Varying the circumferential modulus caused greatest absolute changes in error from the error at the optimized parameter values on the lateral tibial plateau of

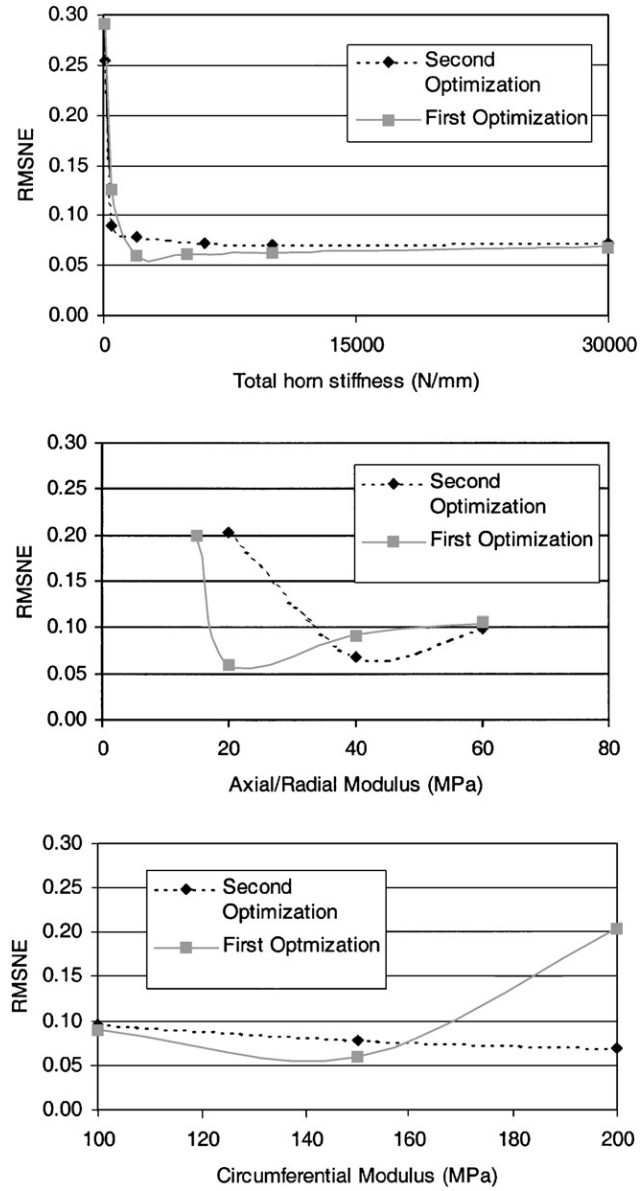

Fig. 3. RMSNE for the three high-sensitivity parameters.

15.6%, 23.8%, and 21.1% for the maximum pressure, mean pressure and contact area, respectively (Table 4). Varying the axial/radial modulus caused greatest absolute changes in error from the error at the

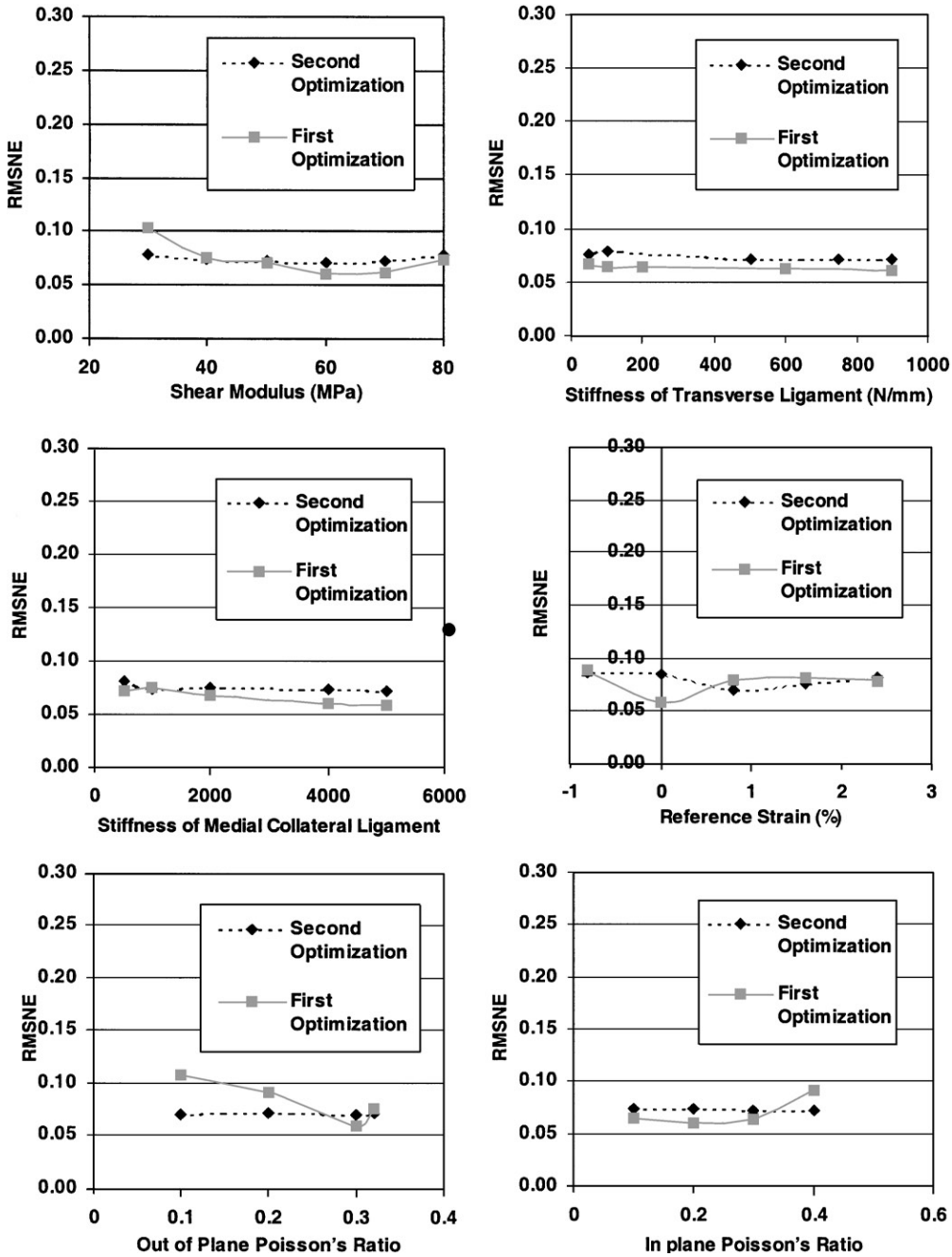

Fig. 4. RMSNE for the six low-sensitivity parameters.

optimized parameter values on the lateral tibial plateau of 21.3%, 19.5%, and 18.7% for the maximum pressure, mean pressure and contact area, respectively (Table 5). Varying the horn stiffness caused greatest absolute changes in error from the error at the optimized parameter values on the lateral tibial plateau of 54.9%, 10.9%, and 7.0% for the maximum pressure, mean pressure and contact area, respectively (Table 6).

The results of the grid search also serve to determine allowable combinations of values of the three most sensitive parameters. For an allowable RMSNE of 10%, many combinations are possible (Table 3). For example, for any value of the circumferential modulus between 100–200 MPa and horn stiffness greater than 6000 N/mm, the axial/radial modulus must be greater than or equal to 40 MPa. These combinations include 67% (12 of 18) of the RMSNE values below 10% in the grid search.

Considering the meniscal tissue to be linearly elastic and isotropic increased the RMSNE substantially

Table 4
Values of contact variables and corresponding errors from the first optimization for variations in the circumferential modulus. Italicized rows indicate optimized values. Positive is medial and anterior for the M/L and A/P locations of maximum pressure, respectively

Circum. modulus (MPa)	Max. pressure (MPa)	Error (%)	Mean pressure (MPa)	Error (%)	Area (mm^2)	Error (%)	A/P location of max. pressure (mm)	M/L location of max. pressure (mm)	Error (%)
Lateral tibial plateau									
Pressure-film data	3.78		1.53		384.8		5.6	−17.6	
100	3.40	10.1	1.46	4.3	409.5	−6.4	5.3	−16.2	−1.3
150	*3.69*	*2.4*	*1.59*	*−3.9*	*378.0*	*1.8*	*5.4*	*−16.2*	*−1.0*
200	4.27	−13.2	1.95	−27.7	297.0	22.8	5.5	−16.1	−0.2
Medial tibial plateau									
Pressure-film data	3.46		1.42		372.0		−3.0	18.9	
100	3.62	−4.8	1.31	7.6	355.5	4.4	−1.5	19.5	4.0
150	*3.44*	*0.4*	*1.36*	*4.0*	*360.0*	*3.2*	*−1.6*	*19.5*	*3.7*
200	3.27	5.5	1.64	−15.8	315.0	15.3	−1.7	19.5	3.4

Table 5
Values of contact variables and corresponding errors from the first optimization for variations in the axial/radial modulus. Italicized rows indicate optimized values. Positive is medial and anterior for the M/L and A/P locations of maximum pressure, respectively

Axial/ radial modulus (MPa)	Max. pressure (MPa)	Error (%)	Mean pressure (MPa)	Error (%)	Area (mm^2)	Error (%)	A/P location of max. pressure (mm)	M/L location of max. pressure (mm)	Error (%)
Lateral tibial plateau									
Pressure-film data	3.78		1.53		384.8		5.6	−17.6	
15	4.49	−19.0	1.88	−23.4	306.0	20.5	5.6	−16.1	−0.1
20	*3.69*	*2.4*	*1.59*	*−3.9*	*378.0*	*1.8*	*5.4*	*−16.2*	*−1.0*
40	3.20	15.2	1.55	−1.4	387.0	−0.6	5.4	−16.2	−1.2
60	3.08	18.4	1.56	−2.3	387.0	−0.6	5.3	−16.2	−1.3
Medial tibial plateau									
Pressure-film data	3.46		1.42		372.0		−3.0	18.9	
15	3.40	1.8	1.63	−15.1	306.0	17.7	−1.6	19.4	3.6
20	*3.44*	*0.4*	*1.36*	*4.0*	*360.0*	*3.2*	*−1.6*	*19.5*	*3.7*
40	3.33	3.7	1.38	2.8	346.5	6.9	−1.7	19.5	3.4
60	3.34	3.3	1.41	0.2	342.0	8.1	−1.8	19.5	3.3

relative to the 5.4% value obtained for the transversely isotropic constitutive relation. The minimum RMSNE was 32% with an elastic modulus of 150 MPa and a Poisson's ratio of 0.3.

Using the values of the nine parameters optimized at a compressive load of 1200 N, the model was independently validated under a 400 N compressive load and 15 degrees of flexion. The RMSNE between the model and the experimental contact variables increased by only 0.2% at 400 N and 15 degrees of flexion relative to the RMSNE at 1200 N and 0 degrees of flexion.

Although the contact variables were relatively insensitive to the stiffness of both the transverse ligament and deep MCL when the parameter values were varied within the ranges specified, it was noted that the RMSNE increased when either of the attachments was absent from the model (i.e. stiffness = 0 N/mm). Therefore, to determine the lower bound for the acceptable stiffness, the sensitivity analysis for these two parameters was extended from the minimum values used in the optimizations to zero. When the transverse ligament stiffness was less than 12.5 N/mm, the sensitivity to this parameter increased and the error approached 10% (Fig. 5). In addition, when the deep MCL nonlinear stiffness parameter was less than 125 N, the sensitivity increased and the RMSNE approached 10% (Fig. 5).

Table 6
Values of contact variables and corresponding errors from the first optimization for variations in the horn stiffness. Italicized rows indicate optimised values. Positive is medial and anterior for the M/L and A/P locations of maximum pressure, respectively

Horn stiffness (N/mm)	Max. pressure (MPa)	Error (%)	Mean pressure (MPa)	Error (%)	Area (mm^2)	Error (%)	A/P location of max. pressure (mm)	M/L location of max. pressure (mm)	Error (%)
Lateral tibial plateau									
Pressure-film data	3.78		1.53		384.8		5.6	−17.6	
50	5.76	−52.5	1.75	−14.9	351.0	8.8	5.1	−16.9	−2.4
500	2.83	25.0	1.56	−2.4	396.0	-2.9	5.4	−16.4	−0.9
2000	*3.69*	*2.4*	*1.59*	*−3.9*	*378.0*	*1.8*	*5.4*	*−16.2*	*−1.0*
5000	3.88	−2.7	1.58	−3.3	378.0	1.8	5.4	−16.1	−0.9
10,000	3.95	−4.5	1.57	−3.0	378.0	1.8	5.4	−16.1	−0.9
30,000	4.09	−8.4	1.56	−2.4	382.5	0.6	5.4	−16.1	−0.7
Medial tibial plateau									
Pressure-film data	3.46		1.42		372.0		-3.0	18.9	
50	3.67	−6.0	1.38	2.6	351.0	5.7	−1.4	19.7	4.1
500	3.46	−0.2	1.38	2.5	351.0	5.7	−1.6	19.5	3.7
2000	*3.44*	*0.4*	*1.36*	*4.0*	*360.0*	*3.2*	*−1.6*	*19.5*	*3.7*
5000	3.43	0.7	1.37	3.3	355.5	4.4	−1.6	19.5	3.7
10,000	3.43	0.8	1.37	3.3	355.5	4.4	−1.6	19.5	3.7
30,000	3.43	0.9	1.37	3.3	355.5	4.4	−1.6	19.5	3.7

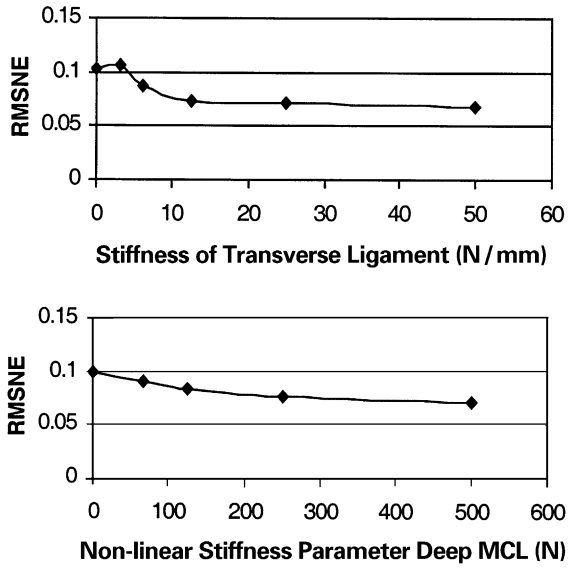

Fig. 5. RMSNE for the transverse ligament and deep medial collateral liagment as parameter values approach zero.

4. Discussion

The purpose of this study was to establish a set of criteria to aid in the design and/or selection of meniscal replacements. To fulfill this purpose, a finite element model of a single cadaveric knee was used in a sensitivity analysis to identify both material and attachment parameters that are the most important determinants of the contact pressure distribution and therefore would influence the long-term success of the replacement. One key finding of this study was that a transversely isotropic, linearly elastic, homogeneous constitutive relation for the meniscal tissue provided a RMSNE as low as 5.4% between the finite element solution and the experimentally determined contact variables. A second key finding was that the model was successfully independently validated using optimized values for both material parameters and attachments. A third key finding was that the contact variables of the tibial plateau are most sensitive to the circumferential modulus, axial/radial modulus, and the total horn stiffness. The contact variables were relatively insensitive to the other six parameters that were examined. A final key finding was that for an axial/radial modulus greater than or equal to 20 MPa, many combinations of the circumferential modulus and total horn stiffness are possible to maintain the contact pressure distribution to within 10% (RMSNE) of the normal knee. Before these findings are discussed further, several methodological issues should be examined because of their possible influence on the interpretation of results.

4.1. Methodological issues

Careful consideration was given to the procedures used for validating the finite element model solution. One important procedural aspect was that a single cadaveric specimen was used to create the finite element model, and the contact pressure distribution was measured in this same specimen. Using a single knee enabled direct comparison of experimental measurements of the contact variables to the contact variables determined from the finite element solution for a given

knee. Inasmuch as there is great variability in the contact variables between knees (Ahmed and Burke, 1983), this provided a stronger validation than constructing a model and then validating it by comparison to contact variables reported in the literature.

A second important procedural aspect was the similarity in the compressive loading and boundary conditions between the model and the experiments. In the previous work (Haut Donahue et al., 2002), the authors demonstrated that the contact solution of the finite element model is strongly influenced by the rotational constraints, with differences in contact variables as large as 19% when rotations other than flexion/extension are constrained. Considering that the load application system applied the compressive load while constraining the flexion angle but allowing freedom of motion in the other two rotations, the model was constrained similarly to insure that the model solution was as relevant to the experiments as possible.

The time of loading during the experiments allowed for an elastic solution to the finite element model. From biphasic theory, the viscoelastic time constant of cartilage is approximately 1500 s (Mow et al., 1991), whereas the joint was compressed in less than 1 s in the experiment. Because fluid does not have time to move for these short loading times, the elastic solution does not deviate from the biphasic solution (Garcia et al., 1998). Therefore, the cartilage can be assumed to behave as an elastic material for the purposes of contact pressure computations (Donzelli et al., 1999). Similarly, the meniscal tissue has a large time constant, on the order of 3300 s (Mow et al., 1991), and can also be treated as an elastic material for compression of the joint during the time of interest.

The anterior and posterior bundles of the deep medial collateral ligament were assumed to have the same values for nonlinear stiffness and reference strain. While others have modeled these bundles with different values of these parameters (Blankevoort et al., 1991; Li et al., 1999; Pandy et al., 1997; Wismans et al., 1980), each of these bundles was assigned the same values to reduce the number of parameters in the optimization. Since the contact variables were not sensitive to either the nonlinear stiffness parameter or the reference strain, this assumption is unlikely to have affected the results.

The value of the in-plane Poisson's ratio was only varied to an upper limit of 0.4. Theoretically, with a transversely isotropic constitutive relation, this value can be as large as 1.0. However, given that little or no sensitivity was evident up to 0.4, it was assumed that increasing the range to the theoretical upper limit of 1.0 would not change the results. In addition, it is important to note that the ranges for the Poisson's ratios used during the optimization did not enforce the nearly incompressible behavior of the meniscal tissue at all iterations, that can be expected for short loading times. However, the values for the Poisson's ratios that resulted from the optimization maintain the near incompressible criterion for the transversely isotropic meniscal tissue.

Because the finite element solution was compared to experimental results, the procedural aspects surrounding the experimental measurement of the contact pressure distribution also merit critical examination. Pressure-sensitive film was used to measure the contact pressure distribution of the tibial plateau. Because this transducer is sensitive to humidity (Ateshian et al., 1994; Martens et al., 1997), temperature (Ateshian et al., 1994), and shear artifact (Ateshian et al., 1994), care was taken to ensure that these sources of error were controlled during the experiment. All of the compression tests were conducted on the same day to control for temperature and humidity. In addition, the joint was distracted to avoid shear artifacts when placing the film into the joint. Despite these efforts, an error ranging from 1.7% to 26% is inherent in the measurement of contact pressure using pressure sensitive film depending on joint geometry, loading, and mechanical properties of the cartilage (Liggins et al., 1992; Wu et al., 1998). With our experimental technique however, we conservatively estimate that the film was accurate to approximately 5% which is comparable to the minimized value of the RMSNE.

Following the procedures noted above, the model was validated by demonstrating that the model contact variables at a different load (i.e. 400 N) and flexion angle (15°) than that for which optimized parameters were determined (i.e. 1200 N and 0 degrees of flexion) gave a comparable RMSNE. This independent validation allows the model to be used with confidence in applications beyond those of interest herein. Such applications would include a sensitivity analysis to both meniscal and bony geometry, as well as placement of the anterior and posterior horns on the tibial plateau.

Notwithstanding that the present study used a single cadaveric knee, the results should apply generally. The overall meniscal width and depth in the transverse plane as well as the cross-sectional dimensions vary between specimens (Haut et al., 2000). Furthermore, the size and shape of both the femur and tibia vary between specimens as well (Elias et al., 1990; Kurosawa et al., 1980; Mensch and Amstutz, 1975; Reostlund et al., 1989). However, the fact that both the circumferential modulus and the axial/radial modulus are two of the three most important determinants of the contact pressure distribution, and these moduli are intrinsic to the material, they independent of geometry and would not be expected to be any less sensitive for different knee specimens. Also the horn stiffness is unrelated to the anatomical variances within a knee specimen.

In evaluating the results of the sensitivity analysis, it was assumed that an increase in the RMSNE of about

5% above the minimum of 5.4% was an important increase. However, to our knowledge no previous research has determined what relative increase in contact variables accelerates the rate of cartilage wear. Nevertheless, some perspective can be gained by recognizing that a 5% difference in contact variables still represents a significant reduction from the changes in the contact variables seen for the meniscectomized knee (Allen et al., 1984; Baratz et al., 1986; Bolano and Grana, 1993; Kurosawa et al., 1980; Rangger et al., 1995). Peak contact pressures on the lateral and medial articular surfaces of the tibia increase over 300% in the meniscectomized knee (Baratz et al., 1986; Kurosawa et al., 1980; Paletta et al., 1997; Seedhom and Hargreaves, 1979), and contact areas decrease by 50% (Baratz et al., 1986; Fukubayashi and Kurosawa, 1980; Kurosawa et al., 1980; Paletta et al., 1997). Thus it is reasonable to assume that changes of only 5% above the baseline minimum of 5.4% would reduce the rate of cartilage wear relative to the rate of the meniscectomized condition.

4.2. Significance of results

The optimization of the nine parameters resulted in a minimization of the RMSNE to 5.4%. This result indicates that a linearly elastic and transversely isotropic constitutive relation of the meniscal tissue provides normal contact pressure distributions and that an orthotropic relation is not necessary. When a linearly elastic and isotropic constitutive relation was used for the meniscal tissue, the RMSNE was never below 32%. Therefore, in future design of meniscal replacements, the material behavior can be transversely isotropic, need not be orthotropic, and should not be isotropic. While an orthotropic material behavior may in fact result in a lower RMSNE, the 5.4% error achieved with the transversely isotropic behavior is sufficient.

Based on the results of the sensitivity analysis, the design and/or selection of meniscal replacements should focus on two material parameters: the circumferential modulus and the axial/radial modulus. Sensitivity of the contact variables to the circumferential modulus was expected based on previous research (Schreppers et al., 1990; Spilker and Donzelli, 1992). However, the finding that the radial/axial modulus is also important is new to this study. Since the meniscus is compressed axially, as well as stressed circumferentially, the sensitivity of the contact pressure distribution to the modulus in the axial direction is not surprising.

Implementing these results in the selection of meniscal replacements will require some developments beyond current practice. Currently, meniscal allografts are selected by tissue banks based upon a geometric match of tibial plateau measurements (L'Insalata et al., 1996), and material parameters are not considered. To improve upon the technique for selecting meniscal allografts, so that they more closely restore the contact variables of the knee joint to normal, the circumferential and axial/radial moduli should be matched as well. To enable this match, techniques should be developed for measuring these two moduli in vivo in the knee of the injured patient. While techniques have been developed to measure the in vivo stiffness of articular cartilage (Lyyra et al., 1995), they have not been applied to measuring the two moduli in a transversely isotropic meniscus. The results of the current study suggest the need to develop such a technique.

The finding that the contact pressure distribution cannot be restored to normal using a linearly elastic and isotropic constitutive relation for the meniscal material leads to a useful requirement in the design and fabrication of replacement menisci. Because an isotropic material will not restore normal contact in the joint, the material used to construct either synthetic or tissue-engineered menisci needs to be transversely isotropic. In view of this requirement, future design efforts should focus on composite materials that exhibit a specified transversely isotropic material response.

Not only were the contact variables sensitive to material parameters, but they were also markedly affected by the attachments, and most notably the stiffness of the horn attachment. When the total stiffness of the horn attachments was less than 2000 N/mm, the RMSNE increased to more than 10% (Fig. 3, Table 3). This confirms previous experimental studies that show attaching horns to the tibial plateau with relatively low stiffness sutures instead of cemented bone plugs causes large differences in contact pressures (Chen et al., 1996). This result also has implications for rehabilitation from meniscal replacement surgery. Because even bone plugs must be anchored by sutures until they are incorporated biologically into the bone plug tunnels, weight bearing of the knee joint should be avoided until the bone plugs become incorporated into the surrounding host bone. Early weight bearing before complete healing of the bone plugs has occurred would lead to potentially detrimental changes in the contact pressure distribution of the knee as a result of lower horn stiffness.

The contact variables were relatively insensitive to both the transverse ligament and deep medial collateral ligament as long as the stiffness of these structures was greater than or equal to 12.5 N/mm for the transverse ligament and 125 N for the medial collateral ligament (Fig. 5). Therefore, the current data suggests that both attachments should be established to restore the contact pressure distribution as closely as possible to normal. In fact, current surgical practice does attempt to restore the boundary condition provided by the deep MCL by suturing the perimeter of the meniscal transplant to the joint capsule during replacement surgery (Miller and

Harner, 1993; Siegel and Roberts, 1993; Stone and Rosenberg, 1993; Veltri et al., 1994), and this study confirms the importance of this suturing. However, the addition of peripheral sutures to cemented bone plugs causes no significant change in contact variables from those with cemented bone plugs alone (Alhalki et al., 1999). Thus, the efficacy of the suturing procedure seems questionable particularly at the time of implantation. However, in vivo studies in both animal models and humans have shown that suturing eventually allows healing of the meniscal perimeter to the joint capsule (Arnoczky et al., 1988; Arnoczky et al., 1990; Jackson et al., 1992; Mikic et al., 1993; Milachowski et al., 1989) which may increase the stiffness of the attachment, hence better restoring the restraint provided by the deep MCL.

On the other hand, current meniscal allograft surgery does not attempt to restore the attachment of the transverse ligament (Miller and Harner, 1993; Siegel and Roberts, 1993; Stone and Rosenberg, 1993; Veltri et al., 1994). The results of this study indicate that the development of surgical techniques that restore this attachment would be worthwhile. Because the stiffness of the attachment need only approach 12.5 N/mm, there is considerable flexibility in the development of surgical techniques to attach the transverse ligament because the necessary stiffness is constrained by only a relatively low bound.

As important as determining the parameters to which the contact variables are sensitive, it is equally important to determine the parameters to which the contact variables are not sensitive. This knowledge will steer future efforts towards controlling the important parameters rather than the unimportant parameters. Neither the shear modulus nor the Poisson ratios were important determinants of the contact pressure distribution for a meniscal replacement in this study. Therefore, these parameters may not need to be as tightly controlled in the design/selection of a meniscal replacement.

Additionally, acceptable ranges (i.e. tolerances) can be identified on the three most sensitive parameters (circumferential modulus, the axial/radial modulus, and the horn stiffness). For an RMSNE below 10%, the circumferential modulus can range from 100 to 200 MPa, the axial/radial modulus can range from 40 to 60 MPa, and the total horn stiffness must be greater than or equal to 6000 N/mm. Some other combinations of the two moduli and horn stiffness are also possible (particularly the optimal combination) (Table 3). Since 17 of the 18 total combinations with RMSNE less than 10% have a horn stiffness greater than 2000 N/mm, the utility of these results depends directly on the value of the horn stiffness. To date, the horn stiffness has not been measured and is unknown. Since this stiffness needs to be known to properly use the results of the tolerance study, determining this stiffness would be worthwhile.

In summary, the results of this study should advance meniscal replacement surgery toward a more quantitatively controlled process. To improve the selection of meniscal allografts so that they more closely restore the normal contact pressure distribution of the knee joint, both the circumferential and axial/radial moduli should be matched as well as the geometry. Since techniques do not exist for measuring these moduli in vivo in injured patients, these techniques should be developed. Furthermore, in the design of synthetic replacements, the biological incorporation should be of concern, as well as the values of the circumferential and axial/radial moduli. With replacement by either an allograft or a synthetic, the results from the current study support the idea that meniscal replacement surgery should attach the horns via a technique that yields high stiffness ($\geqslant$2000 N/mm) and also attach both the transverse and deep medial collateral ligaments via techniques that yield stiffness values of 12.5 N/mm and 125 N for the transverse ligament and medial collateral ligament, respectively. These measures will assure that the important determinants of the contact variables from both materials and boundary conditions standpoint are considered in replacement surgery.

Acknowledgements

The authors are grateful to the Whitaker Foundation for providing the financial support to undertake this project.

Appendix A

Inasmuch as two ranges of film were used to experimentally measure the contact pressure distribution, the mean pressure was determined by combining results from both ranges of film. This required several steps. In the first step, the contact area (A_{SL}) was determined for the super-low-range film and both the contact area (A_L) and mean pressure (P_L) were determined for the low-range film for each trial (Fig. 6). In the second step, the contact pressure for the region of the super-low-range film corresponding to that of the low-range film was set to zero. Next, the mean pressure (P_D) and the contact area (A_D) of the remaining donut-shaped region of interest were calculated (Huang et al., 2002). In the final step, the mean pressure (P) for the composite image was calculated from

$$P = [((P_D \times A_D) + (P_L \times A_L))/(A_L + A_D)]. \quad \text{(A.1)}$$

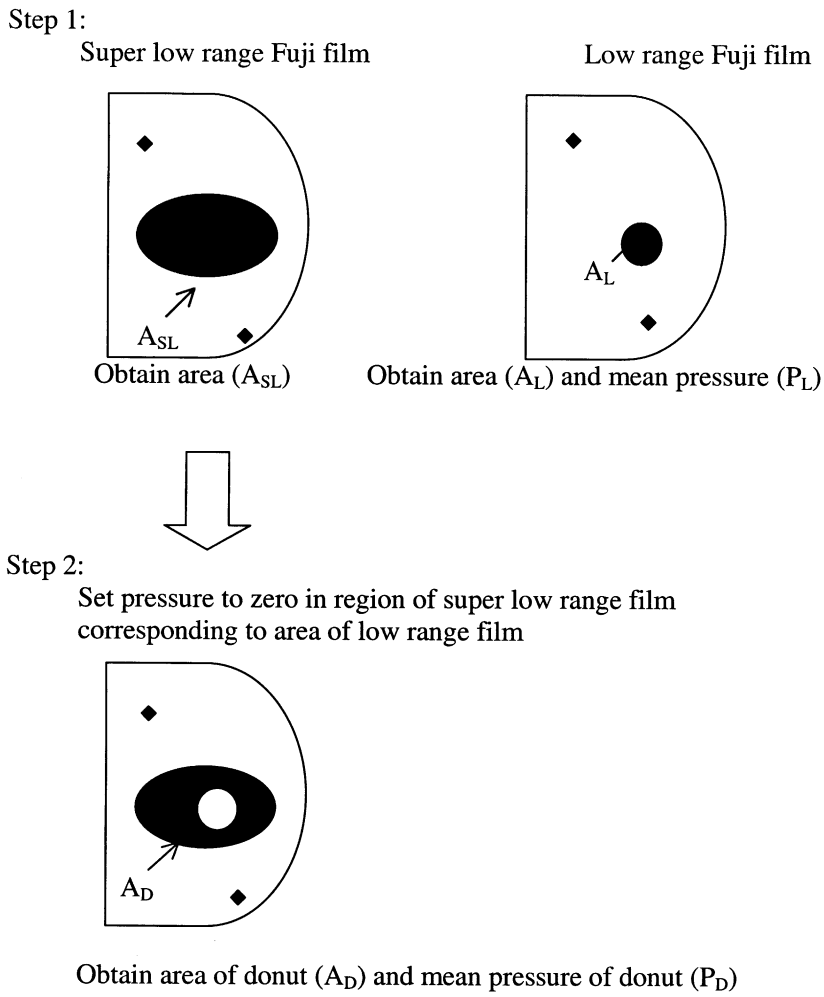

Fig. 6. The technique used to calculate the mean pressure from two ranges of pressure sensitive film.

References

Ahmed, A.M., Burke, D.L., 1983. In-vitro measurement of static pressure distribution in synovial joints—Part I: tibial surface of the knee. Journal of Biomechanical Engineering 105 (3), 216–225.

Alhalki, M.M., Howell, S.M., Hull, M.L., 1999. How three methods for fixing a medial meniscal autograft affect tibial contact mechanics. American Journal of Sports Medicine 27 (3), 320–328.

Allen, P.R., Denham, R.A., Swan, A.V., 1984. Late degenerative changes after meniscectomy. Factors effecting the knee after operation. Journal of Bone and Joint Surgery [Br] 66, 666–671.

Arnoczky, S.P., Adams, M., De Haven, K., Eyre, D., Mow, V., Kelly, M.A., Proctor, C.S., 1987. Meniscus. In: Woo, S.L.Y., Buckwalter, J.A. (Eds.), Injury and Repair of the Musculoskeletal Soft Tissues. American Academy of Orthopaedic Sugeons, Chicago, pp. 487–537.

Arnoczky, S.P., McDevitt, C.A., Schmidt, M.B., Mow, V.C., Warren, R.F., 1988. The effect of cryopreservation on canine menisci: a biochemical, morphologic, and biomechanical evaluation. Journal of Orthopedic Research 6 (1), 1–12.

Arnoczky, S.P., Warren, R.F., McDevitt, C.A., 1990. Meniscal replacement using a cryopreserved allograft: an experimental study in the dog. Clinical Orthopedics and Related Research 252, 121–128.

Ateshian, G.A., Kwak, S.D., Soslowsky, L.J., Mow, V.C., 1994. A stereophotogrammetric method for determining in situ contact areas in diarthrodial joints, and a comparison with other methods. Journal of Biomechanics 27 (1), 111–124.

Bach, J.M., Hull, M.L., 1995. A new load application system for in vitro study of ligamentous injuries to the human knee joint. Journal of Biomechanical Engineering 117 (4), 373–382.

Baratz, M.E., Fu, F.H., Mengato, R., 1986. Meniscal tears: the effect of meniscectomy and of repair on intraarticular contact areas and stress in the human knee. A preliminary report. American Journal of Sports Medicine 14 (4), 270–275.

Berns, G.S., Hull, M.L., Patterson, H.A., 1990. Implementation of a five degree of freedom automated system to determine knee flexibility in vitro. Journal of Biomechanical Engineering 112 (4), 392–400.

Blankevoort, L., Kuiper, J.H., Huiskes, R., Grootenboer, H.J., 1991. Articular contact in a three-dimensional model of the knee. Journal of Biomechanics 24 (11), 1019–1031.

Bolano, L.E., Grana, W.A., 1993. Isolated arthroscopic partial meniscectomy: functional radiographic evaluation at five years. American Journal of Sports Medicine 21 (3), 432–437.

Butler, D.L., Kay, M.D., Stouffer, D.C., 1986. Comparison of material properties in fascicle-bone units from human patellar

tendon and knee ligaments. Journal of Biomechanics 19 (6), 425–432.

Chen, M.I., Branch, T.P., Hutton, W.C., 1996. Is it important to secure the horns during lateral meniscal transplantation? A cadaveric study. Arthroscopy 12 (2), 174–181.

De Boer, H.H., Koudstaal, J., 1991. The fate of meniscus cartilage after transplantation of cryopreserved nontissue-antigen-matched allograft. A case report. Clinical Orthopedics and Related Research 266, 145–151.

Donzelli, P.S., Spilker, R.L., Ateshian, G.A., Mow, V.C., 1999. Contact analysis of biphasic transversely isotropic cartilage layers and correlations with tissue failure. Journal of Biomechanics 32 (10), 1037–1047.

Elias, S.G., Freeman, M.A., Gokcay, E.I., 1990. A correlative study of the geometry and anatomy of the distal femur. Clinical Orthopaedics and Related Research 260, 98–103.

Fauno, P., Nielson, A.B., 1992. Arthroscopic partial meniscectomy: a long term follow-up. Arthroscopy 8 (3), 345–349.

Fithian, D.C., Schmidt, M.B., Ratcliffe, A., Mow, V.C., 1989. Human meniscus tensile properties: regional variation and biochemical correlation. Transactions of ORS 35, 205.

Fukubayashi, T., Kurosawa, H., 1980. The contact area and pressure distribution pattern of the knee. A study of normal and osteoarthrotic knee joints. Acta Orthopedica Scandanavia 51 (6), 871–879.

Garcia, J.J., Altiero, N.J., Haut, R.C., 1998. An approach for the stress analysis of transversely isotropic biphasic cartilage under impact load. Journal of Biomechanical Engineering 120 (5), 608–613.

Garrett, J.C., Stevensen, R.N., 1991. Meniscal transplantation in the human knee: a preliminary report. Arthroscopy 7 (1), 57–62.

Haut, T.L., Hull, M.L., Howell, S.M., 1997. A high accuracy three-dimensional coordinate digitizing system for recontructing the geometry of diarthrodial joints. Journal of Biomechanics 31 (6), 571–577.

Haut, T.L., Hull, M.L., Howell, S.M., 2000. Use of roentgenography and MRI to predict meniscal geometry determined with a three-dimensional coordinate digitizing system. Journal of Orthopedic Research 18, 228–237.

Haut Donahue, T.L., Hull, M.L., Rashid, M.M., Jacobs, C.R., 2002. A finite element model of the human knee joint for the study of tibio-femoral contact mechanics. Journal of Biomechanical Engineering 124 (3), 273–280.

Huang, A.Z., Hull, M.L., Howell, S.M., Haut Donahue, T.L., 2002. Identification of cross-sectional parameters of lateral meniscal allografts that predict tibial contact mechanics in human cadaveric knees. Journal of Biomechanical Engineering, to appear.

Huberti, H.H., Hayes, W.C., 1984. Patellofemoral contact pressures. The influence of *q*-angle and tendofemoral contact. Journal of Bone and Joint Surgery [Am] 66 (5), 715–724.

Jackson, D.W., McDevitt, C.A., Simon, T.M., Arnoczky, S.P., Atwell, E.A., Silvino, N.J., 1992. Meniscal transplantation using fresh and cryopreserved allografts. An experimental study in goats. American Journal of Sports Medicine 20 (6), 644–656.

Kohn, D., Wirth, C.J., Reiss, G., Plitz, W., Maschek, H., Erhardt, W., Wulker, N., 1992. Medial meniscus replacement by a tendon autograft. Experiments in sheep. Journal of Bone and Joint Surgery [Br] 74 (6), 910–917.

Kollias, S.L., Fox, J.M., 1996. Meniscal repair. Where do we go from here? Clinics in Sports Medicine 15 (3), 621–630.

Kurosawa, H., Fukubayashi, T., Nakajima, H., 1980. Load-bearing mode of the knee joint; physical behavior of the knee with or without menisci. Clinical Orthopaedics and Related Research 149, 283–290.

Li, G., Gil, J., Kanamori, A., Woo, S.L., 1999. A validated three-dimensional computational model of a human knee joint. Journal of Biomechanical Engineering 121 (6), 657–662.

Liggins, A.B., Hardie, W.R., Finlay, J.B., 1995. The spatial and pressure resolution of Fuji pressure-sensitive film. Experimental Mechanics 35, 166–173.

Liggins, A.B., Stanart, J.C.E., Finlay, J.B., Rorabeck, C.H., 1992. Calibration and manipulation of data from Fuji pressure-sensitive film. In: Little, E. (Ed.), Experimental Mechanics: Technology Transfer Between High Tech Engineering. Elsevier, New York, pp. 61–70.

L'Insalata, J., Klatt, B., Caravaggio, H., Fu, F., Harner, C.D., 1996. Accuracy and reliability of office techniques for meniscal allograft sizing. Cryolife Corp., Marietta GA.

Lyyra, T., Jurvelin, J., Pitkanen, P., Vaatainen, U., Kiviranta, I., 1995. Indentation instrument for the measurement of cartilage stiffness under arthroscopic control. Medical Engineering and Physics 17 (5), 395–399.

Martens, T.A., Hull, M.L., Howell, S.M., 1997. An in vitro osteotomy to expose the medial compartment of the human knee joint. Journal of Biomechanical Engineering 119 (4), 379–385.

Mensch, J.S., Amstutz, H.C., 1975. Knee morphology as a guide to knee replacement. Clinical Orthopaedics and Related Research 112, 231–241.

Messner, K., 1994. The concept of a permanent synthetic meniscus prosthesis: a critical discussion after 5 years of experimental investigations using dacron and teflon implants. Biomaterials 15 (4), 243–250.

Mikic, Z.D., Brankov, M.Z., Tubic, M.V., Lazetic, A.B., 1993. Allograft meniscus transplantation in the dog. Acta Orthopedica Scandanavia 64 (3), 329–332.

Milachowski, K.A., Weismeier, K., Wirth, C.J., 1989. Homologous meniscus transplantation. Experimental and clinical results. International Orthopedics 13 (1), 1–11.

Miller, M.D., Harner, C.D., 1993. The use of allograft. Techniques and results. Clinics in Sports Medicine 12 (4), 757–770.

Mow, V.C., Zhu, W., Ratcliffe, A., 1991. Structure and function of articular cartilage and meniscus. In: Mow, V.C., Hayes, W.C. (Eds.), Basic Orthopaedic Biomechanics. Raven Press, New York.

Noyes, F.R., Grood, E.S., 1976. The strength of the anterior cruciate ligament in humans and rhesus monkeys. Journal of Bone and Joint Surgery, American Volume 58 (8), 1074–1082.

Paletta, G.A., Manning, T., Snell, E., Parker, R., Bergfeld, J., 1997. The effect of allograft meniscal replacement on intraarticular contact area and pressures in the human knee. American Journal of Sports Medicine 25 (5), 692–698.

Pandy, M.G., Sasaki, K., Kim, S., 1997. A three-dimensional musculoskeletal model of the human knee joint. Part I: theoretical construction. Computer Methods in Biomedical Engineering 1, 87–108.

Rangger, C., Klestil, T., Gloetzer, W., Kemmler, G., Benedetto, L.P., 1995. Osteoarthritis after arthroscopic partial meniscectomy. American Journal of Sports Medicine 23 (2), 240–244.

Reostlund, T., Carlsson, L., Albrektsson, B., Albrektsson, T., 1989. Morphometrical studies of human femoral condyles. Journal of Biomedical Engineering 11 (6), 442–448.

Schreppers, G.J.M.A., Sauren, A.A.H.J., Huson, A., 1990. A numerical model of the load transmission in the tibio-femoral contact area. Journal of Engineering in Medicine 204 (1), 53–59.

Seedhom, B.B., Hargreaves, D.J., 1979. Transmission of the load in the knee joint with special reference to the role of the menisci. Engineering in Medicine 8, 220–228.

Siegel, M.G., Roberts, C.S., 1993. Meniscal allografts. Clinics in Sports Medicine 12 (1), 59–80.

Skaggs, D.L., Warden, W.H., Mow, V.C., 1994. Radial tie fibers influence the tensile properties of the bovine medial meniscus. Journal of Orthopaedic Research 12 (2), 176–185.

Spilker, R.L., Donzelli, P.S., 1992. A biphasic finite element model of the meniscus for stress-strain analysis. In: Mow, V.C., Arnoczky,

S.P., Jackson, D.W. (Eds.), Knee Meniscus, Basic and Clinical Foundations. Raven Press, New York.

Stone, K.R., 1993. Meniscal transplantation using fresh and cryopreserved allografts. American Journal of Sports Medicine 21 (5), 762.

Stone, K.R., Rodkey, W.G., Webber, R., McKinney, L., Steadman, J.R., 1992. Meniscal regeneration with copolymeric collagen scaffolds. In vitro and in vivo studies evaluated clinically, histologically, and biochemically. American Journal of Sports Medicine 20 (2), 104–111.

Stone, K.R., Rosenberg, T., 1993. Surgical technique of meniscal replacement. Arthroscopy 9 (2), 234–237.

Tissakht, M., Ahmed, A.M., 1995. Tensile stress–strain characteristics of the human meniscal material. Journal of Biomechanics 28 (4), 411–422.

Tissakht, M., Farinaccio, R., Ahmed, A.M., 1989. Effect of ligament attachments on the respone of the knee menisci in compression and torsion: a finite-element study. Transactions of ORS 35, 203.

Veltri, D.M., Warren, R.F., Wickiewicz, T.L., SJ, O.B., 1994. Current status of allograft meniscal transplantation. Clinical Orthopeadics 303, 44–55.

Whipple, R., Wirth, C.R., Mow, V.C., 1984. Mechanical Properties of the Meniscus. ASME Advances in Bioengineering, 1984, 32–33.

Wismans, J., Veldpaus, F., Janssen, J., Huson, A., Struben, P., 1980. A three-dimensional mathematical model of the knee joint. Journal of Biomechanics 13 (8), 677–685.

Wu, J.Z., Herzog, W., Epstein, M., 1998. Effects of inserting a pressensor film into articular joints on the actual contact mechanics. Journal of Biomechanical Engineering 120 (5), 655–659.